Colloids and Surfaces A: Physicochemical and Engineering Aspects 695 (2024) 134218

Contents lists available at ScienceDirect

Colloids and Surfaces A: Physicochemical and Engineering Aspects

journal homepage: www.elsevier.com/locate/colsurfa

Environmentally friendly SLIPS coating based on flexible sponge: A novel approach to antifouling for ships

Fengqin Li, Yuxue Hu, Xiaoming feng *, Guizhong Tian *

College of Mechanical Engineering, Jiangsu University of Science and Technology, Zhenjiang 212100, China

HIGHLIGHTS

- Hydrophobic surface with 3D interconnected net-like structures were achieved through a simple immersion process, effectively capturing liquid lubricants and maintaining long-term stability.
- Changing the surface energy of the mixed coating effectively enhances the adsorption capacity for non-polar liquids(oil).
- Prolonged anti-fouling effects by altering the viscosity of injected lubricating oil.

GRAPHICAL ABSTRACT

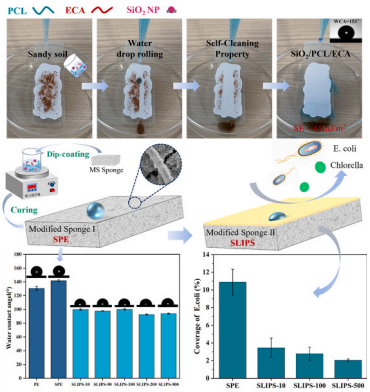

ARTICLE INFO

Keywords:
Slippery surface
SLIPS
Viscosity
Flexible/stretchable coatings
Antifouling

ABSTRACT

To mitigate the attachment of fouling organisms, Slippery Liquid-Infused Porous Surfaces (SLIPS) hold tremendous potential as a green and broad-spectrum antifouling solution, capable of replacing traditional antifouling coatings. However, the complexity of current preparation methods and the limited lifespan of lubricating oils constrain their widespread application in marine antifouling for vessels. In this study, melamine sponge (MS) was used as a substrate, and modifications were made by introducing superhydrophobic silica nanoparticles (SiO_2 NPs), a biocompatible adhesive (ethyl cyanoacrylate, ECA), and a highly stretchable polymer (poly-ε-caprolactone, PCL). By combining natural surface microstructures with additional nanomaterials, we successfully obtained a superoleophilic surface, effectively capturing liquid lubricants and maintaining their long-term stability. The sponge substrate possesses distinctive contractility, with the lubricant stored in the grid spontaneously compensating for the loss of surface lubricant, thereby effectively enhancing its durability. This study provides a straightforward fabrication method with reduced manufacturing costs for environmentally friendly marine anti-fouling coatings. The approach demonstrates a prolonged cyclic anti-fouling effect, effectively advancing the development of SLIPS for anti-fouling applications in shallow marine environments.

* Corresponding authors.
E-mail addresses: xmfeng@just.edu.cn (X. feng), justtgz@163.com (G. Tian).

https://doi.org/10.1016/j.colsurfa.2024.134218
Received 21 February 2024; Received in revised form 17 April 2024; Accepted 6 May 2024
Available online 12 May 2024

1. Introduction

As marine resources are continually exploited, marine biofouling stands out as a significant challenge in the realm of oceanic industrial production and maritime transportation [1,2]. The adhesion, corrosion, and damage caused by marine fouling organisms to underwater equipment significantly increase hydrodynamic resistance, leading to elevated fuel consumption, greenhouse gas emissions, and a shortened lifespan for vessels and equipment [3–7]. Beyond the immediate impact on industry, long-distance marine transportation contributes to the introduction of invasive species, posing a threat to the survival and reproduction of local species in the ecological environment [8]. Given these challenges, minimizing commercial losses caused by biofouling is of paramount importance. Effectively combating marine biofouling not only enhances economic benefits but also reduces energy consumption and safeguards ecosystems.

To date, the most economically effective approach for better resistance against biofouling is achieved by altering the composition and mechanisms of antifouling coatings [9]. Early antifouling coatings primarily utilized toxic biocides in their formulations to inhibit fouling organisms before adhesion and deposition. However, given the adverse effects of biocides on aquatic life and human health [10,11], researchers have dedicated efforts to developing environmentally friendly antifouling strategies. Inspired by the lotus leaf, textured superhydrophobic surfaces (SHS) have been extensively investigated. Trapped air layers within the surface microstructure can impede the adhesion of fouling organisms [12,13]. Nevertheless, most superhydrophobic surfaces face challenges of highly unstable air layers and poor mechanical stability in underwater environments, making them prone to wetting and loss of superhydrophobicity [14–17]. Structural defects can easily lead to the gradual filling of microtextured surfaces by microorganisms such as bacteria or diatoms, thereby compromising antifouling performance.

In recent years, the "Slippery Liquid-Infused Porous Surfaces" (SLIPS) have emerged as an alternative to superhydrophobic surfaces in combating prolonged biofouling due to the superior stability of liquid layers over air layers [18–22]. The continuous and uniform distribution of liquid on SLIPS surfaces provides exceptionally smooth and non-adhesive properties. It enables rapid restoration of liquid repellency after physical damage and can withstand high pressures [1,23,24]. These advantages position SLIPS as having tremendous potential in marine antifouling applications for ships. However, the preparation of porous micro/nanostructures and the storage stability of lubricating liquids still face numerous challenges in practical applications. Specifically, while the produced SLIPS exhibit excellent hydrophobicity, the entire preparation process for forming chemically matched, rough superhydrophobic porous structures is relatively intricate and time-consuming [25–29]. This severely constrains the practical application of SLIPS. Additionally, most reports on SLIPS focus on developing suitable structures on different substrates to accommodate lubricants, with limited research on their long-term durability [30–32]. Due to the complex marine environment, the lubricating liquid of SLIPS cannot exist stably in the long term. After experiencing shear stress in a flow chamber for 7 days, the surface lost a significant amount of lubricant [33]. Therefore, controlling the loss of lubricant under high shear flow is crucial, and the capability to store and replace lubricating oil must meet the application requirements to ensure the practical use of SLIPS.

Considering the long-term presence of porous micro-nano structures in the complex marine environment may lead to a weakening of mechanical performance [34,35]. The preferred method for preparing the SLIPS substrate in this study is to utilize the unique microscale features of the flexible porous melamine sponge surface. The sponge is modified with superhydrophobic nanoparticles (silica nanoparticles, SiO_2 NPs) to achieve extremely low wettability to water. The use of a biocompatible adhesive (ethyl cyanoacrylate, ECA) enhances high adhesion and durability between the substrate and the coating. Simultaneously, a highly stretchable polymer (polycaprolactone, PCL) is chosen to maintain the high elasticity and durability of the coating, ensuring the structural stability of the modified sponge under significant deformations. Through a simple immersion process, a commercially available melamine sponge (MS) is immersed in the mixed solution, followed by drying to achieve solvent evaporation and ECA polymerization. The resulting highly durable, flexible, and stretchable coating can utilize less harmful silicone oil as a substitute for hazardous fluorinated lubricants or expensive siloxane. The coating exhibited outstanding oil-locking capability and durability in various tests. Through simulating marine erosion conditions, we verified that the SLIPS coating also demonstrated excellent antibacterial and antialgal adhesion properties. The entire preparation process is environmentally friendly and efficient, representing a sustainable, fluorine-free alternative and providing valuable insights for the application of SLIPS in the field of antifouling coatings.

2. Experimental section

2.1. Materials

Polycaprolactone (PCL, average Mn = 8w~10w), dichloromethane (DCM, ≥99.5%, containing 50–150 ppm of isoprene stabilizer), ethyl cyanoacrylate (ECA, purity 98%), silica nanoparticles (SiO_2, purity 99.8%, particle size 7–40 nm), and various viscosity grades of dimethyl silicone oil (10, 50, 100, 200, 500 mPa·s) were all obtained from Shanghai Aladdin Bio-Chem Technology Co., Ltd. All reagents were used as received. Chlorella and its culture medium were provided by Haiers Biotechnology Enterprise. Gram-negative Escherichia coli (E. coli, ATCC 25922) was supplied by the Shanghai Collection Center for Industrial Microorganisms. Melamine sponge (MS) was obtained from a local supermarket. Artificial seawater (ASW) was prepared according to ASTM D1141–98 (2013).

2.2. Fabrication of SLIPSs

Polycaprolactone (PCL, 0.9 g) was added to dichloromethane (DCM, 100 mL) and stirred at room temperature for 2 hours until completely dissolved using a magnetic stirrer. Then, hydrophobic SiO_2 NPs (1 g) were added, and the mixture was sonicated for 30 minutes for thorough dispersion. Finally, ethyl cyanoacrylate (ECA, 0.9 g) was added to the solution, and the stirring continued for 2 hours to prepare the coating solution. The pre-cleaned melamine sponge (20 mm × 20 mm × 10 mm) was immersed in the prepared coating solution for 1 minute to ensure complete absorption. The impregnated sponge was then placed on a Buchner funnel connected to a vacuum flask, and excess solvent was removed by vacuum filtration. The remaining solvent was allowed to evaporate at room temperature, followed by crosslinking in a vacuum oven at 60°C for 2 hours. In the subsequent discussion, the sponge modified with SiO_2/PCL/ECA was labeled as SPE, the sponge modified with PCL/ECA as PE, and the sponge modified with SiO_2/ECA as SE. Finally, the samples were immersed in silicone oil of different viscosities for 1 hour and then placed vertically on filter paper for 2 hours to remove excess lubricant. Surfaces lubricated with silicone oil of viscosities 10, 50, 100, 200, and 500 mPa·s were designated as SLIPS-10, SLIPS-50, SLIPS-100, SLIPS-200, and SLIPS-500, respectively.

2.3. Characterization

The surfaces and chemical compositions of the unmodified melamine sponge (MS) and the modified sponge coating (SPE) were characterized using scanning electron microscopy (SEM, Quattro S-type, Thermo Fisher Scientific) and energy-dispersive X-ray spectroscopy (EDS, EDAX ELECT PIUS). Contact angle measurements were performed on the surfaces of PE, SPE, and SLIPSs coatings using a contact angle goniometer (Theta Lite, BIOLINShanghai, China) at room temperature with 5 μL of deionized water. Five measurements were conducted on different

regions of each coating under the same conditions to obtain the average values. The Owens-Wendt method was employed to quantitatively determine the surface energy of the mixed coating based on these measurements. The detailed calculation process and relevant discussions will be elaborated in the Results and Discussion section. The sliding angle (SA) was measured by dropping water droplets onto the surface using a high-speed camera (PCO.dimax S1) at room temperature to determine the surface slipperiness.

2.4. Durability test

To assess the durability of the sponge coating, the oil absorption capacity of the coating was tested using lubricating oil with a viscosity of 50 mPa·s during a repeated adsorption/desorption process. The modified sponge samples were shaped to approximately (20 mm × 20 mm × 10 mm), and the sponge coated with SiO_2/PCL/ECA was immersed in the lubricating oil until reaching absorption equilibrium. After removal, the sample was left to stand on a Büchner funnel for one minute and then weighed. The lubricating oil was manually pressed out of the sponge, and the sponge was reweighed. Three parallel measurements were conducted for each sample. The calculation for mass absorption capacity (Q) is as follows:

$$Q = \frac{(w_1 - w_0)}{w_0} \quad (1)$$

where W_0 and W_1 represent the weights of the sponge before and after oil absorption, respectively.

2.5. Water flow shear test

The modified sponge samples, shaped to dimensions of approximately (20 mm × 20 mm × 10 mm), were immersed in lubricating oils of varying viscosities until no further increase in sample mass was observed. Subsequently, all samples were individually placed in conical flasks containing 50 mL of artificial seawater (ASW). The conical flask was placed in a constant temperature shaking incubator set at 25±1°C, with shaking at a speed of 100 revolutions per minute, during which artificial seawater was replaced once. The initial weight of each sponge, saturated with lubricating oil, was recorded before the experiment (W_s). At intervals of 12 hours, the sponges were removed from the ASW, and all samples were dried at 70°C until no liquid droplets were visible on the surface (W_{dry}). The Relative Weight Loss (WLR) was calculated using the following Eq. (2):

$$WLR = \frac{w_s - w_{dry}}{w_s} \times 100\% \quad (2)$$

For each sample, five parallel measurements were conducted, and the reported weight loss represents the average of these five test values, with the error reported as the standard deviation of the data.

2.6. Lubricant storage stability test

The lubricant storage stability was assessed using the lubricant evaporation loss test (GB 7325–87). The coating samples were immersed in lubricating oil of different viscosities until the sample mass no longer increased. Subsequently, they were placed in an air-drying oven at 100°C. The weight difference between the sponge coatings with injected lubricating oil and those without described the oil absorption of different groups. After gently wiping off excess lubricant from the samples, the weights of different SLIPSs samples were regularly measured and recorded using an electronic analytical balance. The lubricant evaporation loss was calculated based on the weight loss of the samples.

2.7. Bacterial adhesion test

Quantitative analysis of the adherent bacterial count on the coating surface was performed using the plate method. The number of colonies on agar plates reflected the anti-fouling performance of the SLIPSs coating. A shaker box was employed to simulate fluid environments, testing the short-term dynamic anti-fouling performance of the coating. The typical anti-fouling test strain used was Gram-negative Escherichia coli (ATCC 25922). Initially, an inoculation loop was used to collect actively growing E. coli colonies from the agar medium, which were then added to LB liquid medium and cultured for 24 hours at 37°C and 120 rpm. In the next step, three parallel samples were prepared for each type of coating. The coatings were incubated in a bacterial suspension with a turbidity of 0.9 (20 mL) at 37°C for 24 hours with shaking at 100 rpm. Subsequently, the coatings were gently rinsed twice with PBS to remove loosely adhered bacterial cells. The coatings were then placed in a PBS buffer solution and subjected to 20 minutes of ultrasonication. Finally, 5 μL of the sonicated solution was spread on an agar plate and incubated overnight at 37°C. Colonies on the agar plates were observed, and images were captured for colony counting. ImageJ software was utilized to compare the coverage of Escherichia coli on the coating surface.

2.8. Anti-algal settling test

Typical marine microorganisms, such as Chlorella, were selected for the anti-adhesion experiment. Initially, Chlorella solution was added to the F/2 medium and cultured at 25°C in a cultivation chamber with a 12:12 h light-dark cycle using cool white fluorescent light, positioned 50 cm away from the specimens. The concentration of Chlorella solution was estimated at a wavelength of 680 nm using a spectrometer (PG2000-Pro) and labeled as optical density (OD680nm). The coatings were immersed in Chlorella suspension (OD680nm = 0.7) and left static for 24 and 34 days at 25°C (12 h light, 12 h dark). At specific time points, the specimens were gently rinsed with deionized water to remove unattached Chlorella. Finally, fluorescence images of Chlorella were obtained using a fluorescence inverted microscope (DXS-1) to observe the quantity and distribution of algae on the surface, analyzing the adhesion of algae. ImageJ software (version 1.53a) was employed to calculate the number of adhered Chlorella on the coatings. The anti-Chlorella adhesion rate of lubricating oil-injected modified sponges coating relative to the non-oil-injected modified sponges coating was estimated using Formula (3).

$$\text{Anti-chlorella Adhesion Rate (CAR)} = (N_{SPE} - N_{SLIPS}) \div N_{SPE} \times 100\% \quad (3)$$

3. Results and discussion

3.1. Surface characteristics and composition analysis

The morphological and compositional changes of the porous melamine sponge before and after modification are depicted in Fig. 1. Fig. 1 (a) illustrates the microscopic structure of the unmodified sponge, revealing a relatively smooth surface appearance. In Fig. 1(b), the internal microstructure of the sponge after SiO_2/PCL/ECA modification is presented. SEM images show the formation of irregular micro/nanostructures with PCL/ECA and SiO_2 particles within the sponge. The PCL/ECA coating surface exhibits the aggregation of numerous SiO_2 NPs, forming larger clusters. Additionally, it reveals some nanoscale structures, as indicated by the red circles in Fig. 1(b). It is the utilization of the oil storage capacity of the porous microstructure and the oil-capturing effect provided by the nanoscale structures that enables this layered porous internal structure to be more conducive to the formation of SLIPSs than a single-scale smooth surface [17,36].

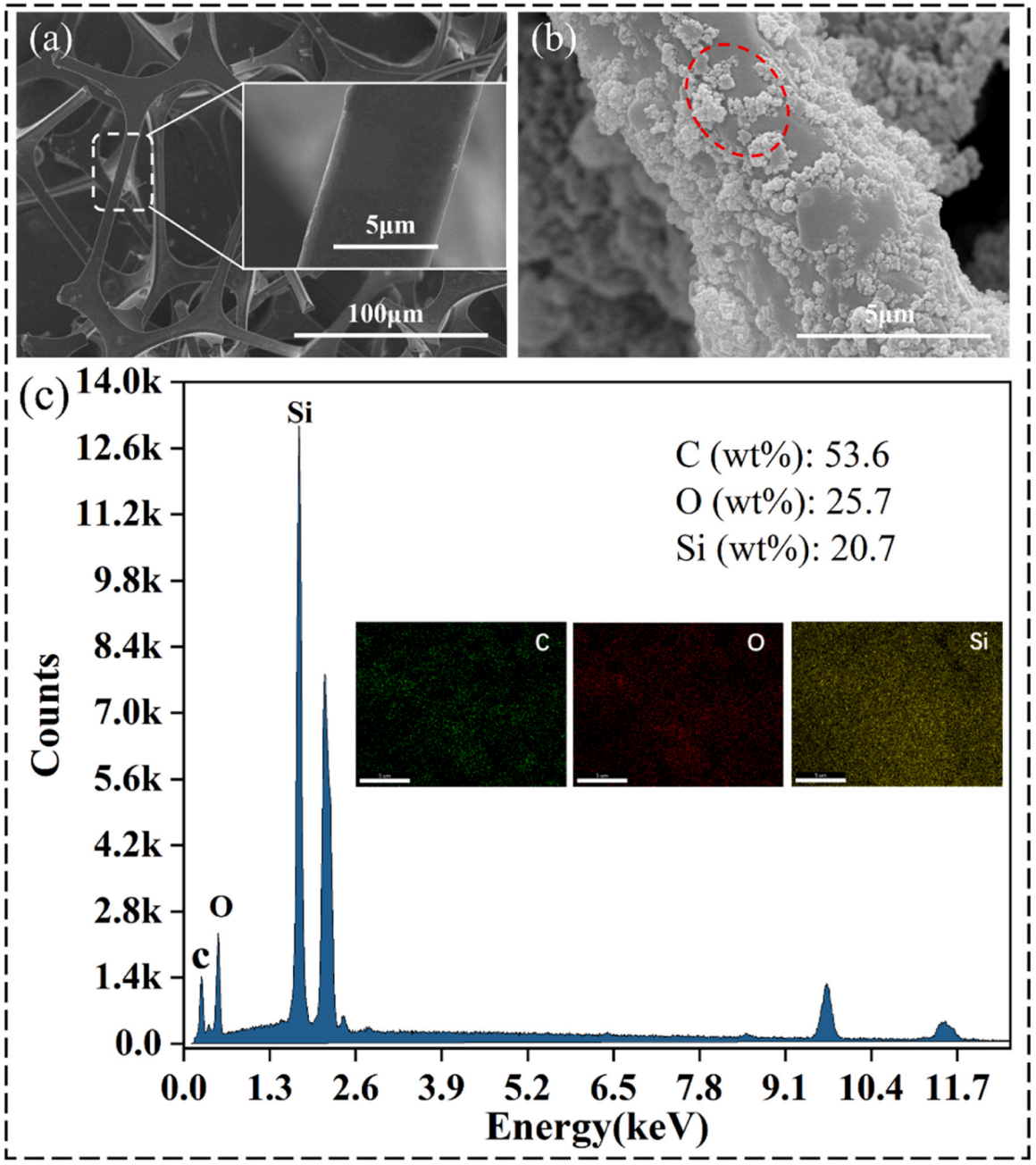

Fig. 1. (a) SEM images of the unmodified sponge coating. (b) SEM image of the modified sponge coating. The red circle indicates SiO_2 NPs embedded in the sponge coating. (c) EDS spectrum of the modified sponge coating (inset shows EDS elemental mapping of C, O, and Si in the modified sponge coating).

In the selection of the primary polymer for the modified sponge coating, priority was given to PCL based on its outstanding flexibility. This flexibility imparts a high degree of elasticity and recoverability to the coating when facing intense motion or impact, a characteristic that was validated in subsequent experiments. Simultaneously, the selection of nanoscale SiO_2 particles provides a fully repellent surface for the coating. Through the adhesive action of the binder and the capillary effect of the sponge itself during the initial impregnation stage, SiO_2 is adsorbed onto the sponge fibers, forming a layer of uniform fine rough structure. This process ensures that the majority of hybrids are formed on the surface of the sponge coating, composed of SiO_2 particles and PCL/ECA, without disrupting the original sponge structure. Fig. 1(c) presents the compositional analysis of the modified material. It is evident from the SEM-EDS elemental mapping and the presence of Si in the EDS spectrum that SiO_2 has been successfully incorporated into the coating. Through effective modification of the sponge coating, not only was the flexibility and elasticity of the coating enhanced but the successful introduction of SiO_2 was also ensured, laying a solid foundation for the comprehensive improvement of coating performance.

3.2. Wettability and roll-off behavior

3.2.1. Modified sponge coating

Through contact angle measurements and anti-adhesion rolling experiments, we conducted detailed testing and characterization of the wettability, self-cleaning, and hydrophobic properties of the measured samples, with specific results shown in Fig. 2.

Fig. 2(a) displays the water contact angle test results for the unmodified sponge, PCL/ECA-modified sponge, and SiO_2/PCL/ECA-modified sponge. In Fig. 2(a1), it can be observed that the water droplet

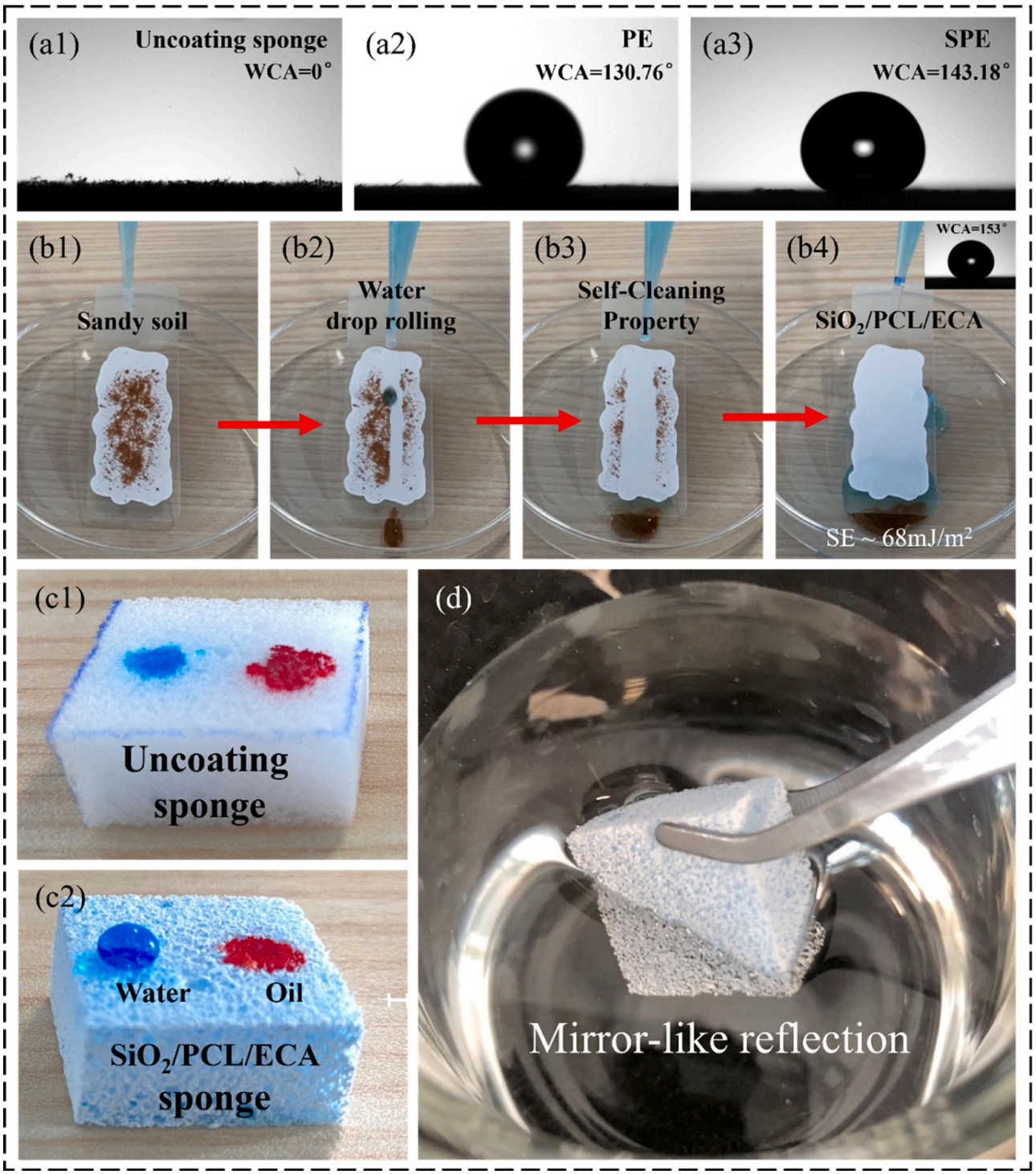

Fig. 2. Water contact angles (WCA) of water droplets on (a1) unmodified sponge, (a2) PCL/ECA sponge, and (a3) SiO_2/PCL/ECA modified sponge coatings. (b1-b4) Self-cleaning performance of coating mixtures. Wetting behavior of water droplets and oil droplets on (c1) unmodified sponge and (c2) SiO_2/PCL/ECA modified sponge coatings. (d)Silver mirror phenomenon.

is completely absorbed within less than 1 s on the unmodified sponge, with a contact angle of 0°, indicating good wettability of the unmodified sponge. However, to successfully use lubricating oil instead of water droplets to wet the substrate, the key is to increase the chemical affinity between the lubricating oil and the substrate. An effective method to enhance chemical affinity is to reduce the surface energy of the substrate by applying a hydrophobic coating, thereby stabilizing the lubricating oil layer on the surface. This study compares two modification schemes, and the contact angle test results of their modified sponge coatings are shown in Fig. 2(a2) and (a3). Compared to the unmodified sponge, the contact angle of the PCL/ECA sponge (Fig. 2(a2)) increased to 130°, showing a certain degree of hydrophobicity. The contact angle of the SiO_2/PCL/ECA sponge (Fig. 2(a3)) further increased to 143°, indicating pronounced hydrophobicity. This is because the successful modification of SiO_2 reduces the surface energy, suggesting that the hydrophobicity of the SiO_2/PCL/ECA sponge is mainly attributed to SiO_2 rather than PCL. In summary, the hydrophobicity of the SiO_2/PCL/ECA-modified melamine sponge may result from the combined effects of the sponge's

porous structure, the micro-nano-level rough structure of the SiO_2 aggregate, and the hydrophobicity of SiO_2 itself.

To further investigate the modified coating, we cast a SiO_2/PCL/ECA mixture film on a glass slide and tested the water contact angle on the SiO_2/PCL/ECA film on the glass slide, showing a result of 153° (see inset in Fig. 2(b4)), demonstrating excellent superhydrophobicity. The glass slide was inclined at an angle of 10°, and sand was used to simulate pollutants to test the anti-adhesion performance of the mixture film. The results in Fig. 2(b1-b4) show that sand is easily carried away by water droplets without leaving any residue, indicating outstanding water-rolling performance and anti-adhesion properties. Therefore, the modified coating mixture exhibits excellent liquid repellency and resistance to contamination adhesion.

Based on evaluating the contact angle and anti-adhesive properties of droplets, the Owens-Wendt method was further employed in this study to test the surface energy of the SiO_2/PCL/ECA coating mixture [37]. Diiodomethane was chosen as the nonpolar liquid, and deionized water was selected as the polar liquid, with known surface tension and polar and dispersive components of the surface free energy (SFE) [38]. This analysis provides a detailed understanding of the surface energy characteristics of the coating, offering robust support for a more comprehensive comprehension of coating performance and wettability.

The surface free energy (SFE) can be determined as shown in Eq. (3):

$$\gamma_S = \gamma_s^d + \gamma_s^p \tag{3}$$

Where γ_S is the SFE, γ_s^d is the dispersion component of SFE and γ_s^p is the polar component of SFE.

Components γ_s^d and γ_S^P of the examined materials may be calculated from[37]

$$\gamma_s^d = \frac{\gamma_D^d(1+COS\theta D)^2}{4} \tag{4}$$

$$\left(\gamma_S^p\right)^{0.5} = \frac{\gamma_w(COS\theta_w+1) - 2\sqrt{\gamma_s^d\gamma_w^d}}{2\sqrt{\gamma_w^p}} \tag{5}$$

Where γ_s^d is the dispersive component of SFE of the examined materials, γ_S^p is the polar component of SFE of the materials examined, γ_D^d is the dispersive component of diiodomethane surface energy, γ_w is the SFE of water, γ_w^d is the dispersive component of water SFE, γ_w^p is the polar component of water SFE, θD is the contact angle of diiodomethane and θ_w is the contact angle of water.

To calculate the SFE of the analyzed materials (SiO_2/PCL/ECA coating mixture), the contact angles θ with the surface of distilled water and diiodomethane were measured. The calculated surface energy of the analyzed material is approximately 68 mJ/m^2, representing an increase of about 44% compared to native PCL (SFE ~38 mJ/m^2). The dispersive component of the analyzed material is approximately 51 mJ/m^2, indicating an increase of about 30% compared to native PCL (~35.8 mJ/m^2). The magnitude of the dispersive component is typically associated with van der Waals forces, which are nonpolar interactions. The affinity of a surface to nonpolar liquids (such as oil) is mainly influenced by nonpolar interactions. Generally, a larger dispersive component indicates a better affinity of the surface to nonpolar liquids. When a surface has a larger dispersive component, van der Waals forces also increase, contributing to an enhanced affinity with nonpolar liquids (oil). This is advantageous for creating oil-repellent surfaces. Therefore, from the perspective of selecting adsorbent materials, the introduction of SiO_2 NPs increases the surface energy of the mixed coating compared to native PCL. This effectively enhances the adsorption capacity for nonpolar liquids (oil), improving the lubricant's wetting effect on the surface. In the subsequent research, we will further modify sponge coatings with such materials and conduct detailed tests on lubricant stability.

Fig. 2(c) contrasts the wetting behavior of untreated sponge (c1) and SiO_2/PCL/ECA-modified sponge (c2) with water droplets and oil droplets. To enhance clarity, bright blue dye was added to the water droplets, and Sudan Red I dye was added to the oil droplets. As observed in Fig. 2 (c1), the untreated sponge rapidly absorbs both water and oil droplets. In contrast, the SiO_2/PCL/ECA-modified sponge presents a spherical shape with the bright blue water droplet, while the red oil droplet is swiftly absorbed by the modified sponge. Submerging the SiO_2/PCL/ECA-modified sponge in water with tweezers results in a mirror-like reflection phenomenon (as shown in Fig. 2d). The appearance of this bright layer is inferred to be caused by the reflection of air between the micro/nanostructure and water [39].

3.2.2. *Modified sponge coating with silicone oil injection(SLIPSs)*

The modified sponge coatings were individually infused with five different viscosity grades of silicone oil (10, 50, 100, 200, and 500 mPa·s), and their water contact angles and roll-off properties were compared, as illustrated in Figs. 3 and 4.

By observing the column chart of water contact angles in Fig. 3, it can be noted that the contact angles of all SLIPSs are relatively stable, maintaining around 96° with minimal fluctuations (<4°). This is because, for SLIPSs, the air layer in the hydrophobic structure is replaced by the infiltrated lubricant, with silicone oil filling the entire porous sponge matrix. This transformation shifts the water contact angle on the surface from a solid-liquid-gas three-phase interface to an oil-water-gas three-phase interface. Compared to the air layer, the lubricant layer demonstrates excellent performance, including stability, durability, defect-free characteristics, and high resistance to humidity [9,36,40]. These attributes are the reasons why SLIPSs can stably exist compared to superhydrophobic surfaces. Additionally, silicone oils are composed of silicon-oxygen-silicon bonds (-Si-O-Si-) and methyl groups attached to silicon atoms. The weak intermolecular interactions between methyl groups contribute to their low surface tension, making them excellent candidates for lubricants [41].

Subsequently, we conducted roll-off tests on the oil-injected modified sponge coating inclined at 10°, and Fig. 4 presents the test results for the 5 SLIPSs samples with different viscosities. It can be observed that water droplets are easily shed from the surface, indicating that the lubricant fills the entire interior of the sponge through capillary action and forms a complete lubricating film covering the substrate surface, thereby significantly reducing the subsequent adhesion of dirt and biological organisms. As the viscosity of the lubricant increases, the sliding speed of droplets on the SLIPSs coating shows a noticeable decrease. This phenomenon arises from the fact that high-viscosity silicone oil has

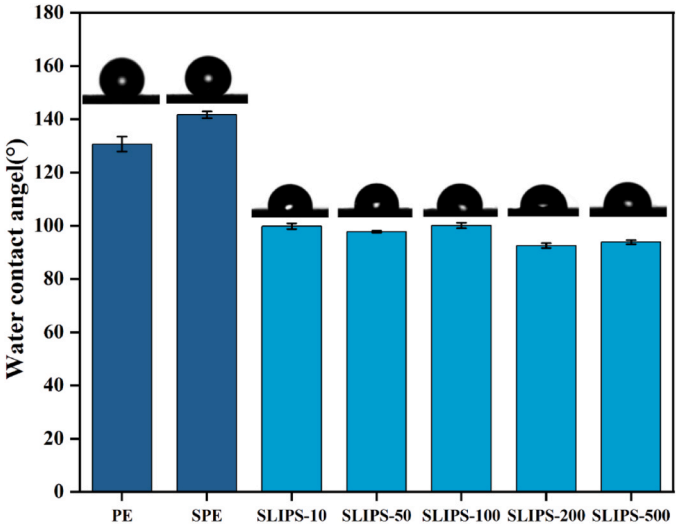

Fig. 3. Water contact angles (WCA) on the surface of modified sponge coatings and oil-injected modified sponge coatings (SLIPSs).

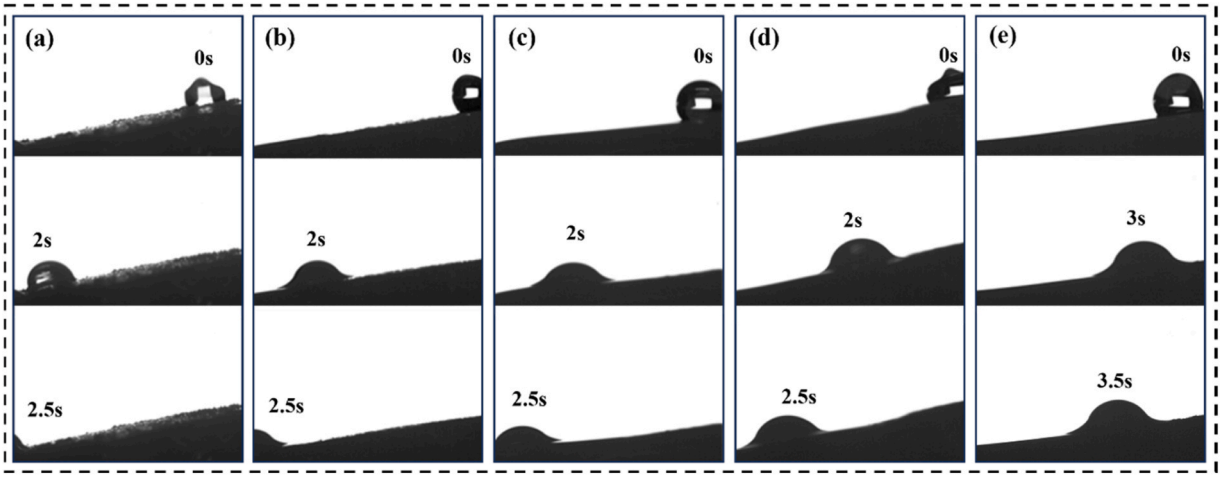

Fig. 4. (a) SLIPS-10, (b) SLIPS-50, (c) SLIPS-100, (d) SLIPS-200, and (e) SLIPS-500, dynamic migration rates of water droplets at a 10° inclination angle on different substrates.

lower deformability, leading to higher viscous resistance (friction). This observation is also documented in previous literature[42]. Considering that rapid slip speeds are typically required in droplet manipulation applications, low-viscosity lubricants are often chosen. However, in the context of the complex marine environment, the stability of the lubricant in SLIPSs coatings becomes one of the crucial properties in the field of ship anti-fouling. To achieve the optimal balance between stability, durability, and slipperiness, it is essential to ensure that the viscosity of the lubricant falls within a moderate range. Therefore, for a comprehensive assessment of lubricant selection criteria, further stability tests and anti-fouling performance evaluations on SLIPSs coatings are necessary.

3.3. Durability

Polycaprolactone (PCL), as an elastic polymer, exhibits excellent fracture toughness. Its strength, toughness, and high resilience confer outstanding seismic resistance, impact resistance, collision resistance, and durability [43]. Its presence in the coating significantly increases elasticity, thereby effectively enhancing the sponge coating's repeatability and recoverability. Additionally, the sponge coated with SiO_2/PCL/ECA demonstrates excellent resistance to large-angle bending, minimizing the likelihood of rupture and almost perfectly restoring its original shape. This indicates that the introduction of PCL into the coating significantly enhances the mechanical performance of the modified sponge without sacrificing its inherent elastic characteristics.

When applying the SiO_2/PCL/ECA modified sponge anti-fouling coating to marine vessels, the influence of water pressure on its reusability and recoverability becomes a critical factor in practical applications. To assess its reusability, cyclic tests were conducted with a maximum of 100 cycles, and the adsorption and oil storage results are presented in Fig. 5(a). During the compression test, the modified sponge rapidly restored its original shape, demonstrating excellent compressibility and elasticity, allowing for repeated use in subsequent oil absorption cycles. From the blue columns in the figure, it can be observed that after 40 adsorption/desorption cycles, the oil absorption slightly decreased (from 19.54 $g{\cdot}g^{-1}$ to 18.52 $g{\cdot}g^{-1}$, a loss of approximately 5%), and then remained relatively stable in the subsequent 100 cycles. In the initial 40 cycles, there was a minor decline in the oil absorption capacity of the modified sponge coating, possibly due to the reduction in available volume caused by the decreased residual oil in the sponge pores, affecting its ability to store lubricating oil.

Furthermore, to demonstrate the importance of PCL in the coating, we conducted the same experiments using a sponge coating covered with SiO_2/ECA (without PCL), and the results are shown in the orange columns in Fig. 5(a). With an increase in the number of cycles, the oil absorption capacity of the sponge exhibited a significant decline. After 40 cycles, the oil absorption loss rate was approximately 13%, which is 2.6 times higher compared to the SiO_2/PCL/ECA modified sponge containing PCL. After 100 adsorption/desorption cycles, the oil absorption capacity decreased from 18.9 $g{\cdot}g^{-1}$ to 15.22 $g{\cdot}g^{-1}$, with a loss of about 19.5%, surpassing the loss rate of the PCL-modified sponge after 100 cycles (~7.5%).

Fig. 5b and (c) respectively present the internal microstructure of the modified sponge coatings after compression/release cycles (excluding lubricating oil). The SEM images reveal that the sponge coated with SiO_2/PCL/ECA (SPE) can bend at a large angle without rupturing and almost perfectly restore its original shape. This indicates that the presence of PCL in the coating significantly enhances the mechanical properties of the modified sponge coating without compromising its elasticity. In contrast, the sponge coated with SiO_2/ECA (SE) exhibited noticeable cracks due to the absence of the elastomer PCL. To visually observe the effect of PCL on the coating, we applied SiO_2/PCL/ECA and SiO_2/ECA coatings on sponge substrates and subjected them to dynamic continuous loading and static weight loading to validate the mechanical properties of the coatings. Initially, uniform pressure testing was conducted using a maximum load of 90 N on samples sized 20 mm × 20 mm × 20 mm. As shown in SI Movie S1, when manually compressed to a volume reduction of over 90%, the sponge in the SPE coating demonstrates remarkable flexibility and resilience. The sponge coated with SE exhibits higher hardness due to the absence of the elastic polymer PCL, accompanied by a significant amount of white powder (SiO_2) around the coating, and poor recovery. Subsequently, we placed 10 N weights individually on the compressed sponge coatings (SI Movie S2), with SPE maintaining its initial form after testing. In contrast, the sponge coated with SE showed that after undergoing a 90 N pressure test, the SiO_2 particles were easily detached from the substrate.

The comprehensive results indicate that the SiO_2/PCL/ECA modified sponge coating, containing PCL, exhibits more stable lubricating oil adsorption performance and superior reusability, allowing it to withstand mechanical impacts and deformations. In contrast, the oil absorption capacity of the modified sponge coating without PCL decreases with the increasing cycles of compression/release. This can be attributed to the hardening of the surface of the sponge coating without PCL, and as the cycles of compression/release increase, the damage to the coating gradually intensifies. This, in turn, leads to the detachment of SiO_2 NPs from the sponge coating, reducing the surface energy of the modified sponge coating, which is unfavorable for the subsequent adsorption of lubricating oil.

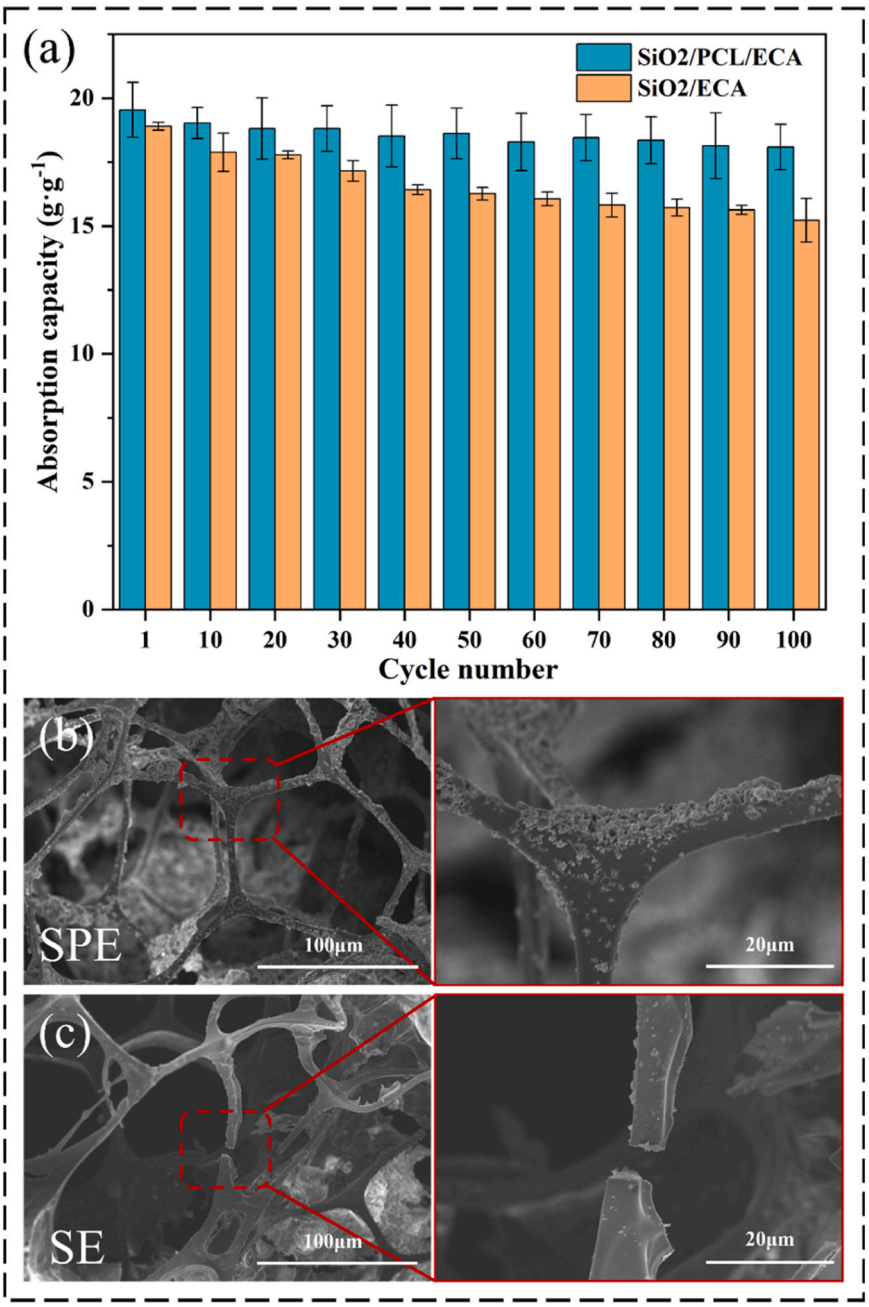

Fig. 5. (a) The oil absorption capacity of SiO_2/ECA modified sponge coating and SiO_2/PCL/ECA modified sponge coating with added PCL as a function of compression cycles. Error bars represent ±SD (n = 3); SEM images of (b) SiO_2/PCL/ECA modified sponge coating and (c) SiO_2/ECA modified sponge coating after compression/release cycles.

3.4. Water flow shear test

As SLIPSs are composed of an oleophilic sponge substrate and lubricating oil with different viscosities, the low adhesion exhibited by the lubricating oil on the sample surface prevents fouling organisms from adhering to the surface when SLIPSs are immersed in seawater. However, with the dynamic processes of seawater and the vessel, along with the complexity of the marine environment, the lubricating oil gradually loses, leading to a reduction in the weight and lifespan of SLIPSs.

As mentioned above, the lifespan of SLIPSs is related to the weight of stored lubricating oil inside the sponge. To estimate the lifespan and mass loss rate of SLIPSs, SLIPSs composed of lubricating oil with different viscosities were placed in continuously oscillating artificial seawater. Periodically, the SLIPSs were removed, and their weights were recorded. The results of the mass loss test are shown in Fig. 6, indicating that the mass loss rate of each SLIPSs coating increases with time. Particularly, the coating with low-viscosity silicone oil (SLIPS-10) shows a mass loss rate exceeding 12% after 240 hours of scouring. In contrast, the mass loss rates for SLIPS-50, SLIPS-100, and SLIPS-200 are relatively small (7.63%, 6.6%, and 5.56%, respectively), demonstrating better stability.

While many lubricants can meet the selection criteria for manufacturing SLIPSs, it is crucial to choose lubricants that meet specific requirements to ensure the long-term stability and durability of SLIPSs. Low-viscosity silicone oil, while easily adsorbed by capillary forces and beneficial for injection into porous structures, is also prone to rapid expulsion from the pores, leading to a significant reduction in

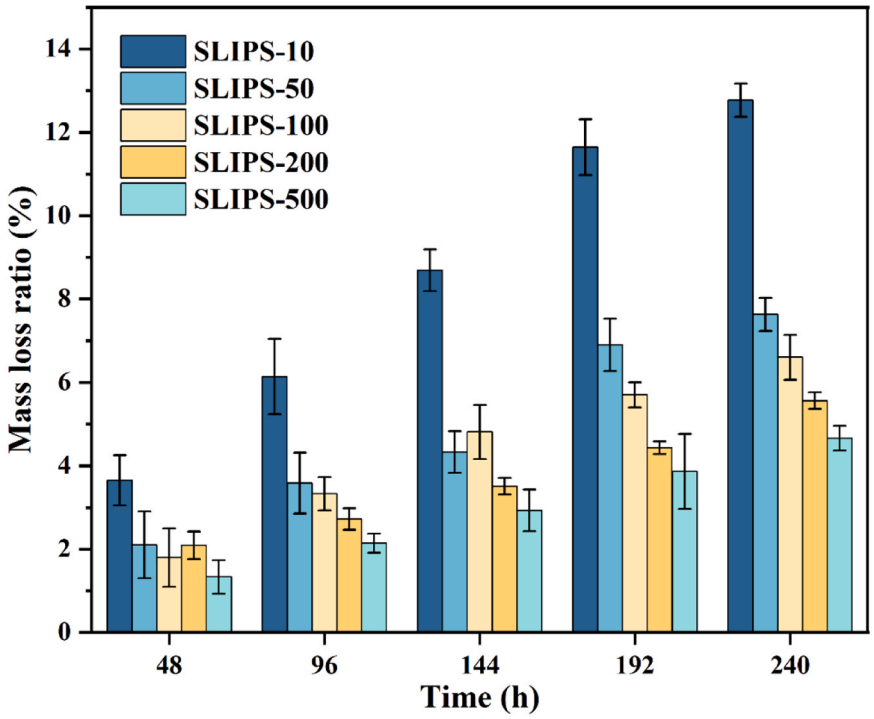

Fig. 6. Mass loss rates of SLIPSs coatings with injected lubricating oils of different viscosities in artificial seawater.

lifespan after flushing. Therefore, it is essential to select silicone oil with an appropriate viscosity as an anti-fouling lubricant for marine applications. The data shows that after 240 hours of flushing, the mass loss rate of SLIPS-500 does not exceed 5%. By using this type of lubricant, lubricant loss can be minimized, enhancing the stability and durability of the coating.

In addition, we attempted to inject higher-viscosity silicone oil into the modified sponge substrate, but the absorption results were not satisfactory. Although high-viscosity silicone oil is the most stable under dynamic conditions of water flow impact and can significantly increase the lifespan of SLIPSs, higher-viscosity silicone oil can affect the absorption efficiency of the coating and hinder the replenishment of subsequent lubricants. Additionally, high-viscosity lubricants facilitate the entanglement of algae, reducing the anti-fouling performance [44]. Therefore, a suitable choice of oil viscosity is essential to achieve good durability while facilitating self-cleaning and self-recovery.

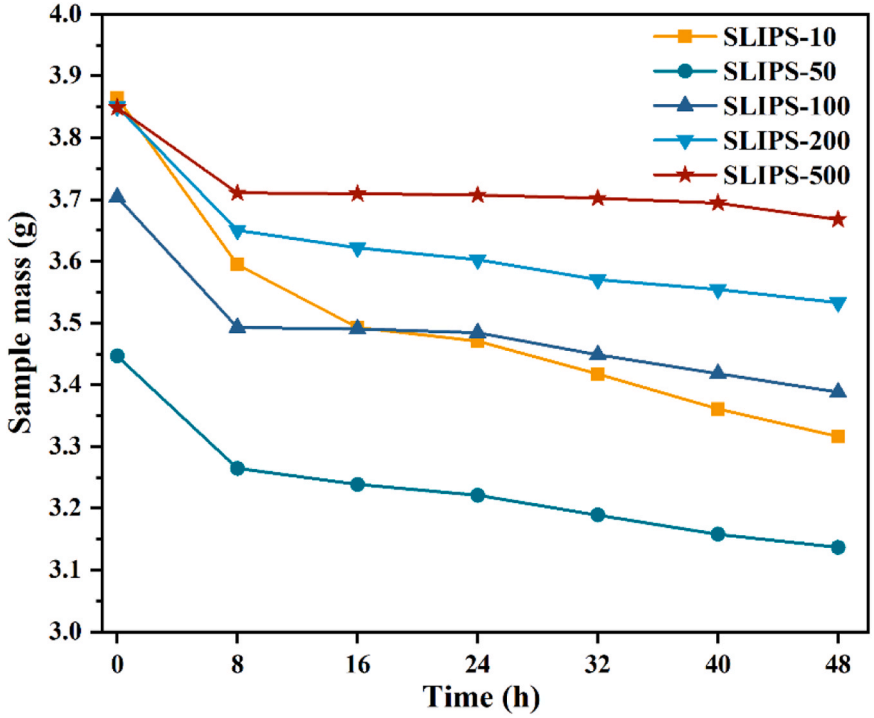

Fig. 7. Mass variation of SLIPSs coatings with injected lubricating oils of different viscosities under constant temperature at 100°C for 48 hours.

3.5. Lubricant storage stability

Due to the unique and advantageous properties conferred by the injected lubricant layer to SLIPSs, the retention of lubricant is indispensable. In addition to monitoring the quality loss of the oil film, we must also focus on the storage stability of the lubricant, which is another key factor influencing the lifespan of the lubricant. To assess the storage stability of the lubricant, SLIPSs immersed in silicone oil with different viscosities were placed in an air-dry oven at 100°C for an accelerated test of lubricant evaporation. The choice of conducting an accelerated test for lubricant evaporation at 100°C instead of employing the current wiping or exhaustion tests is primarily based on the following reasons: Firstly, compared to accelerated tests involving wiping off the lubricant, lubricant evaporation provides a more uniform method that does not cause damage to the surface coating. Secondly, the rate of removing the lubricant through evaporation is faster than the currently used wiping method [45].

The results of the accelerated lubricant evaporation test are shown in Fig. 7, indicating a decrease in the oil film mass of each SLIPSs coating over time, especially within the initial 8 hours. We hypothesize that, during the early stages of the experiment, the surface oil film of the coating samples may not have been sufficiently stable. In the high-temperature environment of 100°C, volatile components in the lubricant are rapidly released into the surrounding atmosphere, resulting in significant initial mass loss. This suggests that, at the beginning of the experiment, the oil film may not have established sufficient stability, leading to the rapid release of volatile components. After 8 hours, the downward trend in oil film mass for each SLIPSs coating gradually becomes more moderate. It is noteworthy that, in the 48-hour oven experiment, compared to the samples with injected high-viscosity silicone oil, the samples with injected low-viscosity silicone oil exhibit a more rapid decline in oil film mass. During this period, the lubricant mass loss rate for SLIPS-10 exceeds 14%. With increasing viscosity of the injected lubricant, the mass loss rates sequentially decrease, with values for SLIPS-50 (9%), SLIPS-100 (8.5%), and SLIPS-200 (8.3%), while SLIPS-500 exhibits a lubricant mass loss rate of only 4.7%.

The reason for this phenomenon is that low-viscosity lubricants have very weak intermolecular forces, making them more prone to leakage from porous structures. In contrast, high-viscosity lubricants have lower fluidity and stronger intermolecular forces, making them less susceptible to loss and conducive to the formation of a stable lubricating layer [44]. Therefore, SLIPS-500 performs better than the other controls in terms of storage stability. Experimental results demonstrate that the higher the viscosity of the injected lubricant on the surface, the better the storage stability of the lubricant, leading to a longer lifespan. Even at high temperatures, increasing viscosity enhances the durability of SLIPSs. The high flowability of liquid lubricants leads to migration, leakage, and depletion, which is detrimental to the lifespan of SLIPSs. Therefore, adopting strategies to improve lubricant retention is crucial.

3.6. Anti-fouling performance

In the process of marine pollution, the most critical step is the formation of a biofilm, involving the predominant participation of bacterial and algal communities[46]. Considering Escherichia coli is one of the most common Gram-negative marine bacteria, inhibiting the initial settling and growth of diatoms can effectively prevent or delay subsequent pollution incidents. Therefore, this study analyzed the antibacterial effect of Escherichia coli using the agar plate method and observed the adhesion state of diatoms on the coating surface through fluorescence microscopy.

The sample coatings were immersed in Escherichia coli bacterial solution and soaked in a fluid environment at 37°C for 24 hours to study their antifouling performance. The bacterial colony count on agar plates was calculated using the spread plate method, and the anti-adhesion effect was quantified through coverage. The specific results are shown in Fig. 8. From Fig. 8(a), it is evident that with the injection of lubricating oil, the number of bacteria on the agar plates decreases, and the anti-bacterial adhesion rate increases, indicating a significant enhancement in the coating's antifouling effect. On the surface of the SPE coating, the coverage rate of Escherichia coli reaches 12.57% (see Fig. 8(a) and (b)), while on the SLIPS surface, the lowest coverage rate of Escherichia coli is only 1.87%. The reason for this difference is that the adhesion behavior of many microorganisms typically occurs only on solid surfaces. The lubricating layer of SLIPS effectively prevents this situation, as Escherichia coli cannot directly contact the solid surface, preventing adhesion to the substrate and thereby inhibiting the formation of a biofilm. Additionally, due to the very low interfacial energy between the lubricating liquid and the substrate, the adhesion work of molecules is significantly reduced, leading to a notable decrease in the adhesion rate[47].

In addition, by comparing Fig. 8(a)(ii), (iii) and (iv), it can be

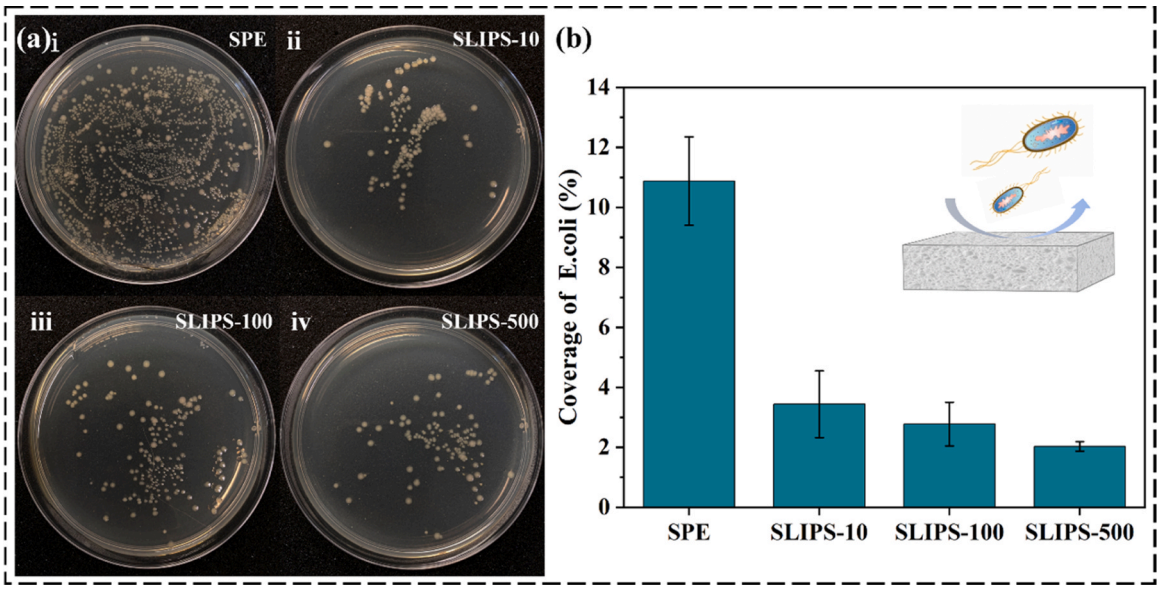

Fig. 8. (a) Diluted agar plate images of colonies produced by Escherichia coli after separation from SLIPSs coatings, i-iv corresponding to un-oiled coating (SPE), SLIPS-10, SLIPS-100, and SLIPS-500, respectively; (b) Surface coverage of Escherichia coli on SLIPSs coatings. Error bars represent ±SD (n=3).

observed that the injection of lubricating oil with different viscosities has a relatively small impact on the adhesion behavior of Escherichia coli. This may be attributed to the relatively short immersion period, during which the lubricating oil remains in a relatively stable state, resulting in no significant differences in the anti-adhesion effects of lubricating oils with different viscosities on the coating. Considering the complexity of the marine environment and the stability of the lubricating oil layer, algal attachment experiments will demonstrate the longer-term antifouling performance.

Fig. 9 shows the fluorescence microscopy images of marine algal contamination on the coating surface and the resistance to algal adhesion. From Figures (a, b, c), it can be observed that after 24 and 34 days of immersion, a large amount of algae coverage is present on the surface of the SPE coating. Due to the three-dimensional interwoven network structure of the SPE surface, its spatial scale is much larger than that of algae, effectively increasing the contact area and making it easy for algae to adhere to the fibers. In contrast, the coated surface after lubricating oil injection shows a trend of low algal coverage, demonstrating good antifouling ability. This is because algae cannot adhere to surfaces with low surface energy [9], so after lubricating oil injection, the number of algae on the surfaces of SLIPS-10, SLIPS-100, and SLIPS-500 decreases compared to the SPE surface. Moreover, with the increase in silicone oil viscosity, the reduction in the number of algae on the coating surface becomes more significant, as evident from Figures (a, b) and Fig. 9(c). However, the change in the number of algae on the SLIPS-10 surface compared to the SPE coating surface is not significant, which may be because, after prolonged immersion, low-viscosity lubricating oil gradually loses. Although silicone oil is chemically inert, molecular diffusion is ongoing, and prolonged contact with the environmental medium leads to lubricating oil loss, ultimately causing the lubricating oil film to fail. In contrast, high-viscosity lubricants have low fluidity, larger intermolecular forces, and are less prone to loss, favoring the formation of a stable lubricating layer. The experimental results further substantiate this point, as evidenced in Fig. 9(c), where the settling density of algae on the surface of the SLIPS-500 coating with 500 mPa·s silicone oil is the lowest.

The resistance to adhesion of Chlorella on the oil-injected SLIPSs coatings is illustrated in Fig. 9(d). After 24 days of immersion, SLIPS-500 exhibits a higher anti-adhesion rate compared to SLIPS-10, reaching 88.73%, a notable increase from 47.89%. Following a 34-day immersion, the coating's resistance to algae adhesion rises from 36.25% for SLIPS-10 to 82.5% for SLIPS-500. Hence, over time, SLIPS-500, characterized by its higher stability, exhibits superior anti-diatom fouling performance.

Taking an overall perspective, within the immersion period of 24–34 days, the settlement of diatoms on the coating surface increases with prolonged immersion time. The SLIPS-500 coating, characterized by its higher stability, demonstrates excellent resistance to diatom fouling throughout the entire process. These results indicate that although silicon oil cannot eradicate algae, it achieves avoidance of fouling through its exceptionally smooth and non-adhesive characteristics, contributing to an environmentally friendly solution. The efficacy

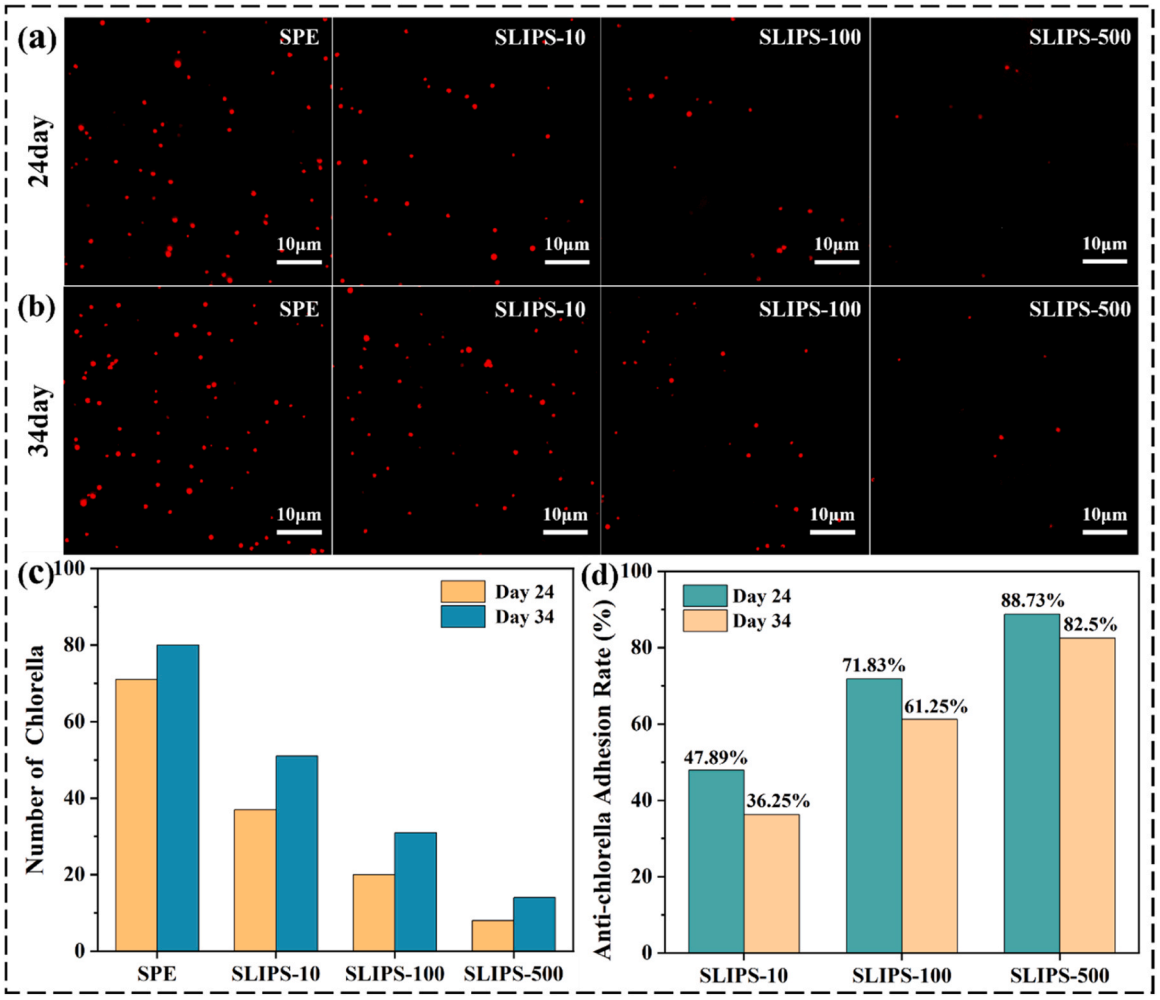

Fig. 9. Fluorescence images of Chlorella settling on SLIPSs coatings after 24 days (a) and 34 days (b). The red dots represent Chlorella. (c) Data showing the settling density of Chlorella on SLIPSs coatings. (d) Anti-chlorella adhesion rate (CAR) of SLIPSs coatings, with the CAR of the un-oiled coating being 0%.

of this anti-fouling performance relies on ensuring the stability of the lubricating oil film, emphasizing the prolonged and more enduring anti-fouling effects when injecting high-viscosity lubricating oil.

4. Conclusions

This study presents a novel design featuring an interconnected network structure of microchannels and cross-linked nanoparticles, serving as a natural reservoir for lubricating oil. This unique structure effectively immobilizes the lubricant, ensuring long-term storage within the network. Experimental evidence has confirmed the vital significance of the designed structure for the storage stability of lubricants when incorporated into liquid-infused porous surfaces (SLIPSs) anti-fouling coatings. Simultaneously, due to the unique characteristics of the sponge, the substrate undergoes slight contraction, leading to the squeezing release of internally stored silicone oil onto the surface, forming a new lubricating layer. This innovative strategy not only enhances the mechanical durability of the surface but also provides a novel approach for the restoration of lubricating performance. In-depth exploration in this domain will contribute to a more comprehensive understanding of the intricate relationships among porous networks, modified materials, viscosity, and the performance of SLIPSs. This research will lay the foundation for the development of more advanced and effective formulations for SLIPSs. This study has opened new avenues for research in SLIPSs anti-fouling coatings, holding the promise to propel the application of SLIPSs in anti-fouling technology and providing valuable insights for the field of materials science.

CRediT authorship contribution statement

Guizhong Tian: Resources. **Xiaoming Feng:** Formal analysis, Conceptualization. **Yuxue Hu:** Writing – review & editing, Writing – original draft. **Fengqin Li:** Validation, Supervision.

Declaration of Competing Interest

The authors declare that they have no known competing financial interests or personal relationships that could have appeared to influence the work reported in this paper.

Data availability

Data will be made available on request.

Acknowledgements

This work was supported by the National Natural Science Foundation of China (No. 52305605 and 52375291), the Natural Science Foundation of the Jiangsu Higher Education Institutions of China (No. 22KJB430022) and the Science Research Project of Jiangsu University of Science and Technology (No. 1022932106).

References

[1] H. Jin, L. Tian, W. Bing, J. Zhao, L. Ren, Bioinspired marine antifouling coatings: Status, prospects, and future, Prog. Mater. Sci. 124 (2022) 100889, https://doi.org/10.1016/j.pmatsci.2021.100889.
[2] X. Liu, J.-L. Yang, D. Rittschof, J.S. Maki, J.-D. Gu, Redirecting marine antibiofouling innovations from sustainable horizons, Trends Ecol. Evol. 37 (2022) 469–472, https://doi.org/10.1016/j.tree.2022.02.009.
[3] A. Ali, M.I. Jamil, J. Jiang, M. Shoaib, B.U. Amin, S. Luo, X. Zhan, F. Chen, Q. Zhang, An overview of controlled-biocide-release coating based on polymer resin for marine antifouling applications, J. Polym. Res 27 (2020) 85, https://doi.org/10.1007/s10965-020-02054-z.
[4] X. Han, J. Wu, X. Zhang, J. Shi, J. Wei, Y. Yang, B. Wu, Y. Feng, Special issue on advanced corrosion-resistance materials and emerging applications. The progress on antifouling organic coating: From biocide to biomimetic surface, J. Mater. Sci. Technol. 61 (2021) 46–62, https://doi.org/10.1016/j.jmst.2020.07.002.
[5] P. Hu, Q. Xie, C. Ma, G. Zhang, Silicone-Based Fouling-Release Coatings for Marine Antifouling, Langmuir 36 (2020) 2170–2183, https://doi.org/10.1021/acs.langmuir.9b03926.
[6] L. Tian, Y. Yin, H. Jin, W. Bing, E. Jin, J. Zhao, L. Ren, Novel marine antifouling coatings inspired by corals, Mater. Today Chem. 17 (2020) 100294, https://doi.org/10.1016/j.mtchem.2020.100294.
[7] X. Wang, Z. Liu, X. Jiang, L. Yu, Self-polishing antifouling coatings based on benzamide derivatives containing capsaicin, Mar. Pollut. Bull. 181 (2022) 113844, https://doi.org/10.1016/j.marpolbul.2022.113844.
[8] Q. Xie, J. Pan, C. Ma, G. Zhang, Dynamic surface antifouling: mechanism and systems, Soft Matter 15 (2019) 1087–1107, https://doi.org/10.1039/C8SM01853G.
[9] D. Li, Z. Lin, J. Zhu, J. Yu, J. Liu, Z. Liu, R. Chen, Q. Liu, P. Liu, J. Wang, An engineering-oriented approach to construct rough micro/nano-structures for anticorrosion and antifouling application, Colloids Surf. A: Physicochem. Eng. Asp. 621 (2021) 126590, https://doi.org/10.1016/j.colsurfa.2021.126590.
[10] Í.B. Castro, F.B. Machado, G.T. de Sousa, C. Paz-Villarraga, G. Fillmann, How protected are marine protected areas: A case study of tributyltin in Latin America, J. Environ. Manag. 278 (2021) 111543, https://doi.org/10.1016/j.jenvman.2020.111543.
[11] M.R.L. Jones, P.M. Ross, Recovery of the New Zealand muricid dogwhelk Haustrum scobina from TBT-induced imposex, Mar. Pollut. Bull. 126 (2018) 396–401, https://doi.org/10.1016/j.marpolbul.2017.11.034.
[12] Y. Cai, W. Bing, C. Chen, Z. Chen, Gaseous Plastron on Natural and Biomimetic Surfaces for Resisting Marine Biofouling, Molecules 26 (2021) 2592, https://doi.org/10.3390/molecules26092592.
[13] S.E. Martins, G. Fillmann, A. Lillicrap, K.V. Thomas, Review: ecotoxicity of organic and organo-metallic antifouling co-biocides and implications for environmental hazard and risk assessments in aquatic ecosystems, Biofouling 34 (2018) 34–52, https://doi.org/10.1080/08927014.2017.1404036.
[14] S.L. Gaw, S. Sarkar, S. Nir, Y. Schnell, D. Mandler, Z.J. Xu, P.S. Lee, M. Reches, Electrochemical Approach for Effective Antifouling and Antimicrobial Surfaces, ACS Appl. Mater. Interfaces 9 (2017) 26503–26509, https://doi.org/10.1021/acsami.7b03761.
[15] M. Sharma, P.K. Roy, J. Barman, K. Khare, Mobility of aqueous and binary mixture drops on lubricating fluid-coated slippery surfaces, Langmuir 35 (2019) 7672–7679, https://doi.org/10.1021/acs.langmuir.9b00483.
[16] M. Xie, W. Zhao, Y. Wu, Preventing algae biofilm formation via designing long-term oil storage surfaces for excellent antifouling performance, Appl. Surf. Sci. 554 (2021) 149612, https://doi.org/10.1016/j.apsusc.2021.149612.
[17] Z. Yang, X. He, J. Chang, C. Yuan, X. Bai, Facile fabrication of fluorine-free slippery lubricant-infused cerium stearate surfaces for marine antifouling and anticorrosion application, Surf. Coat. Technol. 415 (2021) 127136, https://doi.org/10.1016/j.surfcoat.2021.127136.
[18] C. Liu, Y. Li, C. Lu, Y. Liu, S. Feng, Y. Liu, Robust Slippery Liquid-Infused Porous Network Surfaces for Enhanced Anti-icing/Deicing Performance, ACS Appl. Mater. Interfaces 12 (2020) 25471–25477, https://doi.org/10.1021/acsami.0c05954.
[19] X. Liu, X. Gu, Y. Zhou, W. Pan, J. Liu, J. Song, Antifouling Slippery Surface against Marine Biofouling, Langmuir 39 (2023) 13441–13448, https://doi.org/10.1021/acs.langmuir.3c00986.
[20] M. Liu, Z. Gan, B. Jia, Y. Hou, H. Zheng, Y. Wu, S. Li, Z. Guo, Mucilage-inspired robust antifouling coatings under liquid mediums, Chem. Eng. J. 446 (2022) 136949, https://doi.org/10.1016/j.cej.2022.136949.
[21] C. Wei, G. Zhang, Q. Zhang, X. Zhan, F. Chen, Silicone Oil-Infused Slippery Surfaces Based on Sol–Gel Process-Induced Nanocomposite Coatings: A Facile Approach to Highly Stable Bioinspired Surface for Biofouling Resistance, ACS Appl. Mater. Interfaces 8 (2016) 34810–34819, https://doi.org/10.1021/acsami.6b09879.
[22] S. Zhang, X. Liang, X. Teng, G.M. Gadd, J.W. McGrath, C.P. McCoy, Q. Zhao, Enhanced anti-biofilm and anti-protein adsorption properties of liquid-infused silver-polytetrafluoroethylene coatings, Appl. Surf. Sci. 616 (2023) 156463, https://doi.org/10.1016/j.apsusc.2023.156463.
[23] D. Tripathi, P. Ray, A.V. Singh, V. Kishore, S.L. Singh, Durability of slippery liquid-infused surfaces: challenges and advances, Coatings 13 (2023) 1095, https://doi.org/10.3390/coatings13061095.
[24] T.-S. Wong, S.H. Kang, S.K.Y. Tang, E.J. Smythe, B.D. Hatton, A. Grinthal, J. Aizenberg, Bioinspired self-repairing slippery surfaces with pressure-stable omniphobicity, Nature 477 (2011) 443–447, https://doi.org/10.1038/nature10447.
[25] G. Cai, F. Liu, T. Wu, Slippery liquid-infused porous surfaces with inclined microstructures to enhance durable anti-biofouling performances, Colloids Surf. B: Biointerfaces 202 (2021) 111667, https://doi.org/10.1016/j.colsurfb.2021.111667.
[26] J. Chung, H. Cho, H. Yong, D. Heo, Y.S. Rim, S. Lee, Versatile surface for solid–solid/liquid–solid triboelectric nanogenerator based on fluorocarbon liquid infused surfaces, Sci. Technol. Adv. Mater. 21 (2020) 139–146, https://doi.org/10.1080/14686996.2020.1733920.
[27] R. Feng, C. Xu, F. Song, F. Wang, X.-L. Wang, Y.-Z. Wang, A Bioinspired Slippery Surface with Stable Lubricant Impregnation for Efficient Water Harvesting, ACS Appl. Mater. Interfaces 12 (2020) 12373–12381, https://doi.org/10.1021/acsami.0c00234.
[28] S.K. Laney, M. Michalska, T. Li, F.V. Ramirez, M. Portnoi, J. Oh, I.G. Thayne, I. P. Parkin, M.K. Tiwari, I. Papakonstantinou, Delayed Lubricant Depletion of Slippery Liquid Infused Porous Surfaces Using Precision Nanostructures, Langmuir 37 (2021) 10071–10078, https://doi.org/10.1021/acs.langmuir.1c01310.

[29] H. Tran, Y. Kim, C. Ternon, M. Langlet, D. Riassetto, D. Lee, Lubricant Depletion-Resistant Slippery Liquid-Infused Porous Surfaces via Capillary Rise Lubrication of Nanowire Array, Adv. Mater. Inter 8 (2021) 2002058, https://doi.org/10.1002/admi.202002058.

[30] X. Chen, J. Huang, Z. Guo, Stable and biocompatible slippery lubricant-infused anode-oxidated titanium nanotube surfaces *via* a grafted polydimethylsiloxane brush, N. J. Chem. 45 (2021) 17493–17502, https://doi.org/10.1039/D1NJ03465K.

[31] C. Wang, Y. Yan, D. Du, X. Xiong, Y. Ma, WO_3 -based slippery liquid-infused porous surfaces with long-term stability, acsami.0c05315, ACS Appl. Mater. Interfaces (2020), https://doi.org/10.1021/acsami.0c05315.

[32] W. Yao, L. Wu, L. Sun, B. Jiang, F. Pan, Recent developments in slippery liquid-infused porous surface, Prog. Org. Coat. 166 (2022) 106806, https://doi.org/10.1016/j.porgcoat.2022.106806.

[33] N. Keller, J. Bruchmann, T. Sollich, C. Richter, R. Thelen, F. Kotz, T. Schwartz, D. Helmer, B.E. Rapp, Study of Biofilm Growth on Slippery Liquid-Infused Porous Surfaces Made from Fluoropor, ACS Appl. Mater. Interfaces 11 (2019) 4480–4487, https://doi.org/10.1021/acsami.8b12542.

[34] Y.-Y. Quan, Z. Chen, Y. Lai, Z.-S. Huang, H. Li, Recent advances in fabricating durable superhydrophobic surfaces: a review in the aspects of structures and materials, Mater. Chem. Front. 5 (2021) 1655–1682, https://doi.org/10.1039/D0QM00485E.

[35] L. Wang, X. Xiao, E. Liu, S. Yu, X. Yin, J. Wang, G. Zhu, Q. Li, J. Li, Fabrication of superhydrophobic needle-like Ca-P coating with anti-fouling and anti-corrosion properties on AZ31 magnesium alloy, Colloids Surf. A: Physicochem. Eng. Asp. 620 (2021) 126568, https://doi.org/10.1016/j.colsurfa.2021.126568.

[36] Z. Yang, J. Chang, X. He, X. Bai, C. Yuan, Construction of robust slippery lubricant-infused epoxy-nanocomposite coatings for marine antifouling application, Prog. Org. Coat. 177 (2023) 107458, https://doi.org/10.1016/j.porgcoat.2023.107458.

[37] A. Rudawska, E. Jacniacka, Analysis for determining surface free energy uncertainty by the Owen–Wendt method, Int. J. Adhes. Adhes. 29 (2009) 451–457, https://doi.org/10.1016/j.ijadhadh.2008.09.008.

[38] M. Zenkiewicz, J. Golebiewski, S. Lutomirski, Experimental verification of certain van Oss - Good method elements, Polimery 44 (1999) 212–217, https://doi.org/10.14314/polimery.1999.212.

[39] Z. He, H. Wu, Z. Shi, X. Gao, Y. Sun, X. Liu, Mussel-Inspired Durable TiO_2 /PDA-Based Superhydrophobic Paper with Excellent Self-Cleaning, High Chemical Stability, and Efficient Oil/Water Separation Properties, Langmuir 38 (2022) 6086–6098, https://doi.org/10.1021/acs.langmuir.2c00429.

[40] M. Zhang, J. Yu, R. Chen, Q. Liu, J. Liu, D. Song, P. Liu, L. Gao, J. Wang, Highly transparent and robust slippery lubricant-infused porous surfaces with anti-icing and anti-fouling performances, J. Alloy. Compd. 803 (2019) 51–60, https://doi.org/10.1016/j.jallcom.2019.06.241.

[41] S. Peppou-Chapman, J.K. Hong, A. Waterhouse, C. Neto, Life and death of liquid-infused surfaces: a review on the choice, analysis and fate of the infused liquid layer, Chem. Soc. Rev. 49 (2020) 3688–3715, https://doi.org/10.1039/D0CS00036A.

[42] A. Sasidharanpillai, Y. Lee, S. Lee, Design of stable liquid infused surfaces: Influence of oil viscosity on stability, Colloids Surf. A: Physicochem. Eng. Asp. 646 (2022) 128923, https://doi.org/10.1016/j.colsurfa.2022.128923.

[43] W. Li, Y. Zong, Q. Liu, Y. Sun, Z. Li, H. Wang, Z. Li, A highly stretchable and biodegradable superamphiphobic fluorinated polycaprolactone nanofibrous membrane for antifouling, Prog. Org. Coat. 147 (2020) 105776, https://doi.org/10.1016/j.porgcoat.2020.105776.

[44] J. Yuan, Q. Gu, G. Zheng, J. Yang, W. Zhao, Y. Wu, Novel environment-friendly grease-infused porous surface exhibiting long-term cycle effective antifouling performance, Colloids Surf. A: Physicochem. Eng. Asp. 627 (2021) 127196, https://doi.org/10.1016/j.colsurfa.2021.127196.

[45] Y. Li, R. Chen, L. Zhang, Q. Liu, J. Yu, J. Liu, P. Liu, J. Wang, Fabrication and antifouling behavior research of self-healing lubricant impregnated films with dynamic surfaces, Colloids Surf. A: Physicochem. Eng. Asp. 582 (2019) 123865, https://doi.org/10.1016/j.colsurfa.2019.123865.

[46] L. Chen, Y. Duan, M. Cui, R. Huang, R. Su, W. Qi, Z. He, Biomimetic surface coatings for marine antifouling: Natural antifoulants, synthetic polymers and surface microtopography, Sci. Total Environ. 766 (2021) 144469, https://doi.org/10.1016/j.scitotenv.2020.144469.

[47] M. Xie, Y. Wang, W. Zhao, Design novel three-dimensional network nanostructure for lubricant infused on titanium alloys towards long-term anti-fouling, Colloids Surf. B: Biointerfaces 197 (2021) 111375, https://doi.org/10.1016/j.colsurfb.2020.111375.